

Efficient Use of the Spectrum in Small Cell Deployments for 5G Wireless Communications Networks

Sandra Lagen, Adrian Agustin, and Josep Vidal

Universitat Politècnica de Catalunya, Dept. Signal Theory and Communications, Signal Processing and Communications Group, C/ Jordi Girona 1-3 08034 Barcelona (Spain)
Corresponding Author E-mail: {sandra.lagen, adrian.agustin, josep.vidal}@upc.edu

Abstract. *Paired frequency division duplexing (FDD) bands are traditionally adopted at macro cells (MeNBs) but they tend to show inefficient occupancy of the uplink (UL) band due to the asymmetric traffic conditions and prevalence of downlink (DL)-centric applications. To improve spectrum utilization, one possibility is to allow time division duplexing (TDD) small cells (SeNBs) to operate in the underutilized FDD-UL spectrum. However, under an opportunistic access, TDD SeNBs might reuse the same resources as the FDD MeNB to receive in UL and, hence, strong interferences may appear. In this paper, we investigate advanced transmit coordination strategies to allow interference decoding and suppression at the MeNB such that the macro user signal can be decoded interference-free. We propose a novel technique to limit the maximum transmission rate of TDD SeNBs as a function of their distance to the MeNB in a way such that interference decoding and suppression is feasible. Simulation results show that sum-rate gains are obtained when the SeNB is close to the MeNB or when the SeNB transmits at high power (i.e. high interference conditions) as compared to a fully opportunistic access, while the proposed approach allows maintaining normal MeNB operation.*

Key words: flexible duplexing, paired FDD bands, asymmetric traffic conditions, interference decoding and suppression, transmit coordination.

1. Introduction

The almost universal adoption of advanced smartphones has produced a direct impact on the technical requirements of cellular networks, which have been compelled to improve spectral efficiency and spectrum utilization of wireless systems in order to satisfy the increased traffic demands generated by mobile users. The common technical solution adopted worldwide was the use of paired bands under frequency division duplexing (FDD) at macro cells (MeNB), which allocate the same amount of spectrum for both downlink (DL) and uplink (UL) communications. However, due to the overwhelming advent of data services, which are usually predominated by DL-centric applications [1] and impose large traffic asymmetries between DL and UL [2], the conventional paired FDD solution becomes highly spectrally inefficient.

One of the envisioned solutions to improve spectral efficiency and spectrum utilization is to densify the network with small cells (SeNBs), so that the spectrum can be spatially reused [3]. As FDD-based networks with a preassigned paired spectrum tend to have a large amount of unused resources in the FDD-UL band, such resources could be efficiently exploited if multiple time division duplexing (TDD) SeNBs are allowed to operate in the underutilized UL spectrum of an FDD MeNB [4]. Current 3GPP LTE standard and regulation do already hamper the use of these unused resources for DL transmission [5].

The FDD MeNB and TDD SeNBs can access the licensed FDD-UL bandwidth through different access methods: orthogonal or non-orthogonal. Under orthogonal access, MeNB and SeNBs are coordinated to use different time/frequency resources, hence avoiding co-channel interference but requiring of a tight coordination and a proper system configuration [6][7]. An overview of regulation, LTE standardization issues, and different technical solutions based on orthogonal access are provided in [4]. A simpler access is the non-orthogonal one, in which SeNBs are allowed to employ all the resources in the FDD-UL band and hence the MeNB and SeNBs might interfere each other, as shown in Figure 1. Here, we focus on the non-orthogonal access in the underutilized FDD-UL band.

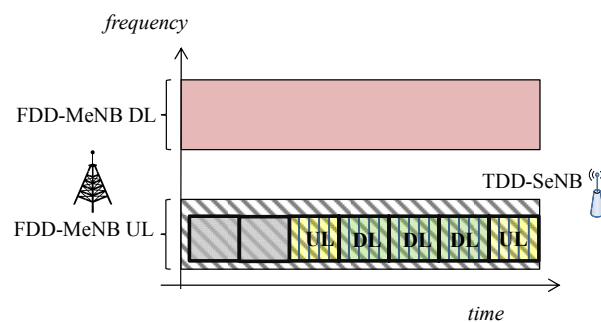


Figure 1. Non-orthogonal access between MeNB and SeNB in the licensed bandwidth for FDD-UL.

Under non-orthogonal access, the main impairment is the co-channel interference generated due to the simultaneous operation of the macro users (MUEs) and the transmissions in TDD mode of either the SeNB or its small users (SUEs). In particular, the most harmful interference situation appears when the SeNB transmits in DL because of the likely line-of-sight (LOS) condition between SeNB and MeNB, which generates DL-to-UL interference from the SeNB towards the MeNB that is receiving in UL. In this context, this paper investigates advanced coordinated strategies and interference mitigation techniques so as to deal with the predominant DL-to-UL interference when shared access in the FDD-UL band is attempted.

A well-known technique to deal with strong interference conditions is the interference decoding and suppression strategy, which has been extensively analyzed in literature and standardization bodies, see [8][9]. For example, 3GPP LTE investigated advanced receivers in the study item “Network-Assisted Interference Cancellation and Suppression (NAICS)” [8], in which all receivers belonging to the family of Interference Cancellation (IC) receivers are based on interference decoding and suppression. The key idea is that the receiver employs a non-linear receive filter to *decode* data symbols of the received interference and then *subtract* it from the received signal, and does so successively until decoding of the useful signal is done interference-free. Also, under dynamic TDD systems, 3GPP LTE analyzed through the study item “enhanced Interference Management and

Traffic Adaptation (eIMTA)” [9] the so-called Interference Suppressing Interference Mitigation strategy (ISIM), where interference decoding and suppression is considered for suppressing one or more dominant DL-to-UL interfering signals in a dynamic TDD system.

Decoding data symbols of the interferer can be performed provided that the interfering signal is received with an acceptable signal-to-interference-plus-noise ratio (SINR). On the other hand, for interference subtraction, perfect knowledge of the interfering channel is required. In this sense, all previous works ([8][9] and references therein) have dealt with the design and evaluation of the receiver capabilities to decode and suppress interference. Differently, in this paper, we will devise a coordinated transmission strategy that will allow a feasible implementation of interference decoding and subtraction.

We focus on the situation in which the FDD MeNB is receiving in UL and the TDD SeNB is transmitting in DL in the FDD-UL band to improve spectrum usage, as shown in Figure 2. In this scenario, interference decoding and suppression would ideally allow: *i*) decoding at the MeNB the data symbols transmitted by the interferer (i.e. the SeNB), *ii*) subtracting them from the received signal at the MeNB, and then *iii*) decoding the useful signal (received from the MUE) at the MeNB without interference. It is important to note that, thanks to the static positions of MeNB and SeNBs, the propagation channel between MeNB and SeNBs can be accurately estimated because of the long coherence time. This suggests that decoding of the data symbols sent by the SeNB is possible at the MeNB. However, not only channel estimation is required for interference decoding and suppression but also the SeNB should transmit at a rate that allows decoding of the interference at the MeNB. A key observation in this respect is that if the SeNB transmits at its maximum rate to serve its associated nearby user, usually this corresponds to a rate higher than the one that can be decoded at the MeNB due to the close SeNB-SUE distance. In this sense, we investigate procedures to limit the transmission rate at the SeNBs for DL transmissions in such a way that the data symbols sent by the SeNB can be properly decoded at the MeNB and, hence, efficient interference decoding and subtraction is permitted.

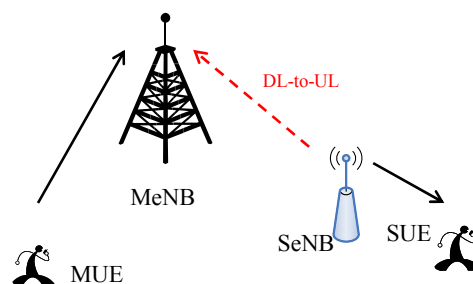


Figure 2. Target scenario composed of a MeNB receiving in UL and a SeNB transmitting in DL. Interference suppression will be implemented at the MeNB to decode and subtract the signal received from the SeNB.

The paper is organized as follows. Section 2 introduces the system model and the signal model. Then, in Section 3 we present the proposed transmit coordination strategy to allow decoding and subtraction of the interference at the MeNB. In Section 4, a statistical analysis is performed and analytical expressions for the maximum rate allowed at the SeNB and the attained rates on each link are derived. Section 5 includes the simulation results. Extension to the case of multiple TDD SeNBs accessing the FDD-UL band is analyzed in Section 6. Finally, conclusions are drawn in Section 7.

2. System model

Consider a paired FDD MeNB with underutilized spectrum in the FDD-UL band due to asymmetric traffic conditions. Assume TDD SeNBs are allowed to transmit/receive in the FDD-UL band to achieve better spectrum utilization through non-orthogonal access (i.e. there is no coordination in terms of the employed resources by the MeNB and the SeNBs, and so they may transmit on the same frequency/time resources simultaneously). We concentrate on a target scenario in which a SeNB transmits in DL and the MeNB receives in UL in the licensed FDD-UL band, as shown in Figure 2. Extension to the case of multiple TDD SeNBs is analyzed in Section 6.

In this setting, high DL-to-UL interference is generated from the SeNB towards the MeNB, see Figure 2. It is important to note two specific characteristics of the target scenario:

- without interference management, the signal from the MUE is received with a low SINR at the MeNB due to the strong DL-to-UL interference received from the SeNB with likely LOS condition.
- the signal from the SeNB is received in average with higher SINR at the SUE than at the MeNB due to the small SeNB-SUE distance.

The former can be addressed if the MeNB is able to decode and suppress the signal from the SeNB, such that the signal from the MUE could be decoded interference-free. The latter happens in all configurations even if LOS appears between SeNB and MeNB, because of the small distance between the SeNB and its SUE. Therefore, if we want to implement interference decoding and suppression at the MeNB (i.e. if we want the MeNB to decode the data symbols sent by the SeNB), then we need to redefine the SeNB transmit strategy so as to make possible decoding of the SeNB data symbols at the MeNB. Note that in case that the SeNB transmits at the highest rate towards its SUE, then data symbols sent by the SeNB may not be decoded by the MeNB because the achievable rate in the SeNB-to-MeNB link might be lower than the rate adopted at the SeNB for DL transmission. One way to allow the decoding is through the limitation of the transmission rate that is permitted at the SeNB to access the FDD-UL band. This is the main idea that will be proposed and analyzed in next sections. But, before proceeding, let us present the signal model.

The received signal at the MeNB and the SUE are, respectively:

$$\begin{aligned} y_{\text{MeNB}} &= g_{\text{MUE-MeNB}} \sqrt{P_{\text{MUE}}} x_{\text{MUE}} + g_{\text{SeNB-MeNB}} \sqrt{P_{\text{SeNB}}} x_{\text{SeNB}} + n_{\text{MeNB}} \\ y_{\text{SUE}} &= g_{\text{SeNB-SUE}} \sqrt{P_{\text{SeNB}}} x_{\text{SeNB}} + g_{\text{MUE-SUE}} \sqrt{P_{\text{MUE}}} x_{\text{MUE}} + n_{\text{SUE}} \end{aligned} \quad (1)$$

where x_{MUE} , x_{SeNB} are the signals transmitted by the MUE and the SeNB, respectively, P_{MUE} , P_{SeNB} denote the transmitted power at the MUE and the SeNB, respectively, g_{z-w} denotes the complex channel gain (including path-loss, shadowing, and fast fading) between the z -th terminal and the w -th terminal (where z, w refer to MeNB, SeNB, MUE, or SUE), and n_{MeNB} , n_{SUE} denote the complex circularly symmetric Gaussian noise components received at MeNB and SUE, respectively, with zero mean and variance σ^2 .

Under the scenario shown in Figure 2, the MeNB is interested in decoding x_{MUE} while the SUE is interested in decoding x_{SeNB} . In the SUE case, due to the close SeNB-SUE distance and low

probability of LOS between MUE and SUE (i.e. low probability of interference), the signal can be properly decoded in general. In contrast, the MeNB can be in trouble for decoding x_{MUE} because of the high levels of received interference due to likely LOS condition between SeNB and MeNB. Therefore, it is convenient to decode the SeNB signal at the MeNB and suppress it from the received signal.

In case that no interference decoding and suppression is performed at the MeNB, and under the assumption that interference is treated as Gaussian noise, the achievable rate of the MUE (for UL) and the SUE (for DL) are:

$$\begin{aligned} R_{\text{MUE-MeNB,int}} &= \log_2(1 + \text{SINR}_{\text{MUE-MeNB}}), \quad \text{SINR}_{\text{MUE-MeNB}} = \frac{|g_{\text{MUE-MeNB}}|^2 P_{\text{MUE}}}{|g_{\text{SeNB-MeNB}}|^2 P_{\text{SeNB}} + \sigma^2} \\ R_{\text{SeNB-SUE}} &= \log_2(1 + \text{SINR}_{\text{SeNB-SUE}}), \quad \text{SINR}_{\text{SeNB-SUE}} = \frac{|g_{\text{SeNB-SUE}}|^2 P_{\text{SeNB}}}{|g_{\text{MUE-SUE}}|^2 P_{\text{MUE}} + \sigma^2} \end{aligned} \quad (2)$$

Assuming that the channel $g_{\text{SeNB-MeNB}}$ is perfectly acquired at the MeNB and interference decoding and suppression is performed at the MeNB, the processed received signal for MUE's signal decoding would be free of interference:

$$\tilde{y}_{\text{MeNB}} = y_{\text{MeNB}} - g_{\text{SeNB-MeNB}} \sqrt{P_{\text{SeNB}}} x_{\text{SeNB}} = g_{\text{MUE-MeNB}} \sqrt{P_{\text{MUE}}} x_{\text{MUE}} + n_{\text{MeNB}} \quad (3)$$

To allow decoding of the SeNB's data symbols at the MeNB (i.e. to allow obtaining the processed signal in (3)), our proposal is to limit the transmission rate at the SeNB. If said rate is not limited, then in most of the cases the MeNB would not be able to properly decode the SeNB signal if maximum rate is used at SeNB, and the achievable rates under interference conditions shown in (2) would be obtained.

4. Transmit Coordination Strategy

As previously mentioned, the signal from the SeNB is received in average with higher SINR at the SUE than at the MeNB. Therefore, our proposal is to limit the SeNB's transmission rate such that the SeNB signal can be decoded at the MeNB. This way, the MeNB could implement decoding and suppression of the interference, and then decode the MUE signal free of interference.

Let us denote by R_{SeNB} the transmission rate selected at the SeNB for DL transmission. On the other hand, the achievable rate for decoding the SeNB signal at the MeNB is:

$$R_{\text{SeNB-MeNB}} = \log_2(1 + \text{SINR}_{\text{SeNB-MeNB}}), \quad \text{SINR}_{\text{SeNB-MeNB}} = \frac{|g_{\text{SeNB-MeNB}}|^2 P_{\text{SeNB}}}{|g_{\text{MUE-MeNB}}|^2 P_{\text{MUE}} + \sigma^2} \quad (4)$$

In case that $R_{\text{SeNB}} \leq R_{\text{SeNB-MeNB}}$, then the MeNB is able to decode the signal received from the SeNB, subtract it from the received signal (as shown in (3)), and perform decoding of the MUE signal interference-free. Otherwise, if $R_{\text{SeNB}} > R_{\text{SeNB-MeNB}}$, then interference decoding is not possible.

Our proposal is to limit R_{SeNB} such that in a specific percentage of the situations (e.g. 90%) the SeNB signal can be decoded at the MeNB. Thus, in average, in 90% of the cases interference suppression is successful while in 10% of the cases the SeNB transmitted data symbols cannot be decoded at the MeNB.

By limiting the SeNB transmission rate in this way, we obtain the following:

- the MUE signal at the MeNB can be decoded interference-free in most of the cases (e.g. 90%), but
- the achievable rate of the SUE to access the licensed FDD-UL band is constrained.

Therefore, a clear trade-off arises. Depending on the MeNB-SeNB distance, LOS conditions, and transmit power of the SeNB, the limitation on the SeNB transmission rate might be either very strong or light (e.g. if the SeNB is far enough from the MeNB then R_{SeNB} would be very low, while if the SeNB is close to the MeNB then R_{SeNB} would be high and hence the MUE could be decoded interference-free while the rate of the SUE would be not much reduced as compared to its maximum rate).

In case of ideal decoding and $R_{\text{SeNB}} \leq R_{\text{SeNB-MeNB}}$, the achievable rate for the MUE (for UL) is interference-free:

$$R_{\text{MUE-MeNB,no-int}} = \log_2(1 + \text{SNR}_{\text{MUE-MeNB}}), \quad \text{SNR}_{\text{MUE-MeNB}} = \frac{|g_{\text{MUE-MeNB}}|^2 P_{\text{MUE}}}{\sigma^2} \quad (5)$$

Note, however, that if $R_{\text{SeNB}} > R_{\text{SeNB-MeNB}}$ then the SeNB signal cannot be decoded at the MeNB and hence the rate for the MUE would be given by the one with interference shown in (2). On the other hand, the achievable rate for the SUE (for DL) is given by the minimum between the rate of the link and the rate imposed by the proposed transmission scheme:

$$R_{\text{SeNB-SUE}} = \min(R_{\text{SeNB}}, \log_2(1 + \text{SINR}_{\text{SeNB-SUE}})) \quad (6)$$

being $\text{SINR}_{\text{SeNB-SUE}}$ shown in (2).

5. Statistical Analysis

In this section we characterize analytically the SeNB rate limitation expression (R_{SeNB}) and the rate expressions of the system as a function of the SeNB-MeNB distance ($d_{\text{SeNB-MeNB}}$) and the SeNB transmitted power (P_{SeNB}) for the proposed transmit coordination strategy that allows interference decoding and suppression presented in Section 4.

To perform the analysis, we adopt the following channel model: $|g_{z-w}|^2 = \frac{1}{kd_{z-w}^\alpha} |h_{z-w}|^2$, where h_{z-w} stands for the fast fading component in the z - w link and kd_{z-w}^α includes pathloss and shadowing losses (being them proportional to the distance between z -th and w -th terminals: d_{z-w}). For simplicity of the presentation, for the linear term k and the pathloss exponent α , we use subindex 1 to denote the SeNB-MeNB link, subindex 2 to refer to the MUE-MeNB link, subindex 3 for the SeNB-SUE link, and subindex 4 for the MUE-SUE link.

5.1. Rate limitation for SeNB

According to this channel characterization, we perform an analysis based on outage probabilities. The outage probability for interference decoding given that the SeNB transmits at a rate R_{SeNB} is:

$$P_{\text{out}} = \Pr\{R_{\text{SeNB-MeNB}} < R_{\text{SeNB}}\}, \quad R_{\text{SeNB-MeNB}} = \log_2 \left(1 + \frac{|h_{\text{SeNB-MeNB}}|^2 P_{\text{SeNB}} / (k_1 d_{\text{SeNB-MeNB}}^{\alpha_1})}{\sigma^2 + |h_{\text{MUE-MeNB}}|^2 P_{\text{MUE}} / (k_2 d_{\text{MUE-MeNB}}^{\alpha_2})} \right) \quad (7)$$

where $\Pr\{a < b\}$ denotes the probability of a being smaller than b .

We assume that the SeNB-to-MeNB channel parameters are known at the MeNB and that $|h_{\text{MUE-MeNB}}|^2 = \gamma$ is an exponential random variable with mean $\bar{\gamma} = E\{|h_{\text{MUE-MeNB}}|^2\}$, being $E\{\cdot\}$ the expectation operator. We also consider that UL power control is adopted at MUEs to transmit towards the MeNB (a typical assumption in 3GPP LTE), such that the ratio $c_2 = P_{\text{MUE}} / (k_2 d_{\text{MUE-MeNB}}^{\alpha_2})$ is fixed. This way, the outage probability in (7) is reduced to:

$$\begin{aligned} P_{\text{out}} &= \Pr \left\{ \log_2 \left(1 + \frac{(P_{\text{SeNB}} / d_{\text{SeNB-MeNB}}^{\alpha_1}) c_1}{\sigma^2 + c_2 \gamma} \right) < R_{\text{SeNB}} \right\} \\ &= \Pr \left\{ (P_{\text{SeNB}} / d_{\text{SeNB-MeNB}}^{\alpha_1}) c_1 - (2^{R_{\text{SeNB}}} - 1) \sigma^2 - (2^{R_{\text{SeNB}}} - 1) c_2 \gamma < 0 \right\} \end{aligned} \quad (8)$$

where $c_1 = |h_{\text{SeNB-MeNB}}|^2 / k_1$. By solving the inequality in (8) and using the fact that γ is an exponential random variable with mean $\bar{\gamma}$, we have:

$$P_{\text{out}} = \int_{\gamma_0}^{\infty} \frac{1}{\bar{\gamma}} e^{-x/\bar{\gamma}} dx = e^{-\gamma_0/\bar{\gamma}}, \quad \gamma_0 = \frac{(P_{\text{SeNB}} / d_{\text{SeNB-MeNB}}^{\alpha_1}) c_1 - (2^{R_{\text{SeNB}}} - 1) \sigma^2}{(2^{R_{\text{SeNB}}} - 1) c_2} \quad (9)$$

If we set an outage probability of P_{ε} , i.e. $P_{\text{out}} = e^{-\gamma_0/\bar{\gamma}} = P_{\varepsilon}$ in (9), then we obtain:

$$\frac{(P_{\text{SeNB}} / d_{\text{SeNB-MeNB}}^{\alpha_1}) c_1 - (2^{R_{\text{SeNB}}} - 1) \sigma^2}{(2^{R_{\text{SeNB}}} - 1) c_2 \bar{\gamma}} = \ln(1/P_{\varepsilon}) \quad (10)$$

Finally, by developing the expression in (10), we get the relation between the maximum rate allowed at the SeNB (R_{SeNB}) and its transmitted power (P_{SeNB}) and the distance to the MeNB ($d_{\text{SeNB-MeNB}}$):

$$R_{\text{SeNB}} = \log_2 \left(1 + \frac{(P_{\text{SeNB}} / d_{\text{SeNB-MeNB}}^{\alpha_1}) c_1}{\sigma^2 + \ln(1/P_{\varepsilon}) c_2 \bar{\gamma}} \right) \quad (11)$$

We can observe in (11) that the rate limitation directly depends on the ratio $P_{\text{SeNB}} / d_{\text{SeNB-MeNB}}^{\alpha_1}$. Therefore, increasing the SeNB transmitted power P_{SeNB} increases the maximum rate allowed at the SeNB R_{SeNB} . On the other hand, increasing the MeNB-SeNB distance $d_{\text{SeNB-MeNB}}$ decreases the maximum rate allowed at the SeNB R_{SeNB} .

Remark 1: If UL power control is adopted at users, the rate limitation for SeNB transmission shown in (11), which guarantees a feasible successive interference decoding and suppression statistically, does not depend on the specific MUE that is scheduled at the MeNB because c_2 in (11) is fixed.

Remark 2: If UL power control is not adopted at users, then the derivation is valid for a rate limitation at the SeNB that depends on the MUE scheduling (i.e. on the specific MUE that is scheduled at the MeNB, since c_2 in (11) would vary with the MUE). Thus, a coordinated scheduling at MeNB and SeNB could be derived with the objective that, depending on the MUE that is scheduled at the MeNB, the SeNB transmits towards a SUE that meets the maximum allowed rate. Otherwise, if we want to make the rate limitation independent of the specific MUE that is scheduled, then we should average over the statistics of the pathloss values for different MUEs.

5.2. Characterization of the average rates

To perform an analytic characterization of the average rates, let us assume that MUE-MeNB, SeNB-SUE, and MUE-SUE fast fading link gains follow an exponential random variable with mean equal to $\bar{\gamma}$, i.e. $\bar{\gamma} = E\{|h_{\text{MUE-MeNB}}|^2\} = E\{|h_{\text{SeNB-SUE}}|^2\} = E\{|h_{\text{MUE-SUE}}|^2\}$. Also assume that SeNB-SUE, MUE-SUE, and MUE-MeNB distances are uniformly distributed random variables with a known mean: $E\{d_{\text{MUE-MeNB}}\} = d_2$, $E\{d_{\text{SeNB-SUE}}\} = d_3$, $E\{d_{\text{MUE-SUE}}\} = d_4$ (in meters). In the present analysis we compute the average rates of the users in the target scenario depicted in Figure 2 based on the average SINR received on each link. Two different strategies are compared:

- ‘INT’: interference situation of a fully opportunistic access, whereby interference is simply treated as Gaussian noise.
- ‘SIC’: transmit coordination strategy proposed in Section 4, in which a maximum rate is allowed at the SeNB and interference decoding and suppression is applied at MeNB.

Under ‘INT’ strategy, the average sum-rate is given by:

$$SR^{\text{int}} = R_{\text{MUE-MeNB}}^{\text{int}} + R_{\text{SeNB-SUE}}^{\text{int}} \left\{ \begin{array}{l} R_{\text{MUE-MeNB}}^{\text{int}} = \log_2 \left(1 + E \left\{ \frac{|h_{\text{MUE-MeNB}}|^2 P_{\text{MUE}} / (k_2 d_{\text{MUE-MeNB}}^{\alpha_2})}{\sigma^2 + (P_{\text{SeNB}} / d_{\text{SeNB-MeNB}}^{\alpha_1}) c_1} \right\} \right) \\ R_{\text{SeNB-SUE}}^{\text{int}} = \log_2 \left(1 + E \left\{ \frac{|h_{\text{SeNB-SUE}}|^2 P_{\text{SeNB}} / (k_3 d_{\text{SeNB-SUE}}^{\alpha_3})}{\sigma^2 + |h_{\text{MUE-SUE}}|^2 P_{\text{MUE}} / (k_4 d_{\text{MUE-SUE}}^{\alpha_4})} \right\} \right) \end{array} \right. \quad (12)$$

By averaging the SINR over the different random variables (fast fading link gains and distances), the rates are thus given by:

$$\begin{aligned} R_{\text{MUE-MeNB}}^{\text{int}} &= \log_2 \left(1 + \frac{\bar{\gamma} P_{\text{MUE}} / (k_2 d_2^{\alpha_2})}{\sigma^2 + (P_{\text{SeNB}} / d_{\text{SeNB-MeNB}}^{\alpha_1}) c_1} \right) \\ R_{\text{SeNB-SUE}}^{\text{int}} &= \log_2 \left(1 + \frac{\bar{\gamma} P_{\text{SeNB}} / (k_3 d_3^{\alpha_3})}{\sigma^2 + \bar{\gamma} P_{\text{MUE}} / (k_4 d_4^{\alpha_4})} \right) \end{aligned} \quad (13)$$

Under ‘SIC’ strategy, the average sum-rate computed by averaging the SINR over the fast fading link gain and distance random variables is given by:

$$SR^{sic} = R_{MUE-MeNB}^{sic} + R_{SeNB-SUE}^{sic}$$

$$\left\{ \begin{array}{l} R_{MUE-MeNB}^{sic} = (1 - P_\varepsilon) \log_2 \left(1 + \frac{\bar{\gamma} P_{MUE} / (k_2 d_2^{\alpha_2})}{\sigma^2} \right) + P_\varepsilon \log_2 \left(1 + \frac{\bar{\gamma} P_{MUE} / (k_2 d_2^{\alpha_2})}{\sigma^2 + (P_{SeNB} / d_{SeNB-MeNB}^{\alpha_1}) c_1} \right) \\ R_{SeNB-SUE}^{sic} = \min \left(\log_2 \left(1 + \frac{(P_{SeNB} / d_{SeNB-MeNB}^{\alpha_1}) c_1}{\sigma^2 + \ln(1/P_\varepsilon) c_2 \bar{\gamma}} \right), \log_2 \left(1 + \frac{\bar{\gamma} P_{SeNB} / (k_3 d_3^{\alpha_3})}{\sigma^2 + \bar{\gamma} P_{MUE} / (k_4 d_4^{\alpha_4})} \right) \right) \end{array} \right. \quad (14)$$

Note that the SeNB transmission rate has been limited in such a way that the MUE-MeNB transmission is interference-free with probability $(1 - P_\varepsilon)$, while there is a probability of P_ε to receive interference from the SeNB at the MeNB. On the other hand, the rate for SeNB transmission is given by the minimum between the average rate on the SeNB-SUE link and the maximum rate imposed by the proposed coordinated transmission scheme.

Therefore, we are interested in comparing the average sum-rates under ‘INT’ and ‘SIC’ strategies as a function of the ratio $X = P_{SeNB} / d_{SeNB-MeNB}^{\alpha_1}$:

$$SR^{int}(X) = \log_2 \left(1 + \frac{\bar{\gamma} P_{MUE} / (k_2 d_2^{\alpha_2})}{\sigma^2 + X c_1} \right) + \log_2 \left(1 + \frac{\bar{\gamma} P_{SeNB} / (k_3 d_3^{\alpha_3})}{\sigma^2 + \bar{\gamma} P_{MUE} / (k_4 d_4^{\alpha_4})} \right)$$

$$SR^{sic}(X) = (1 - P_\varepsilon) \log_2 \left(1 + \frac{\bar{\gamma} P_{MUE} / (k_2 d_2^{\alpha_2})}{\sigma^2} \right) + P_\varepsilon \log_2 \left(1 + \frac{\bar{\gamma} P_{MUE} / (k_2 d_2^{\alpha_2})}{\sigma^2 + X c_1} \right) \quad (15)$$

$$+ \min \left(\log_2 \left(1 + \frac{X c_1}{\sigma^2 + \ln(1/P_\varepsilon) \bar{\gamma} P_{MUE} / (k_2 d_2^{\alpha_2})} \right), \log_2 \left(1 + \frac{\bar{\gamma} P_{SeNB} / (k_3 d_3^{\alpha_3})}{\sigma^2 + \bar{\gamma} P_{MUE} / (k_4 d_4^{\alpha_4})} \right) \right)$$

It can be observed in (15) that:

- $SR^{int}(X)$ is a **decreasing** function of $X = P_{SeNB} / d_{SeNB-MeNB}^{\alpha_1}$, i.e. increasing the SeNB transmitted power or decreasing the SeNB-MeNB distance involves a reduction of the sum-rate due to the increased level of interference received at the MeNB.
- $SR^{sic}(X)$ is the sum of an increasing function (the SUE rate is) and a decreasing function (the MUE rate) with respect to $X = P_{SeNB} / d_{SeNB-MeNB}^{\alpha_1}$. However, the predominant term is the one of the SUE (the MUE-MeNB transmission would receive interference with probability P_ε , e.g. only in the 10% of the cases), such that in general $SR^{sic}(X)$ in (15) is an **increasing** function of $X = P_{SeNB} / d_{SeNB-MeNB}^{\alpha_1}$.

According to this, a threshold for $X = P_{SeNB} / d_{SeNB-MeNB}^{\alpha_1}$ on which ‘INT’ is better than ‘SIC’ in terms of average sum-rate can exist. Note, however, that the proposed coordinated strategy can not only outperform a fully opportunistic access in the FDD-UL band (i.e. ‘INT’ strategy) but also allows the MeNB to maintain its usual operation in the FDD-UL band (i.e. as it was the only one there) while the ‘INT’ strategy can be very detrimental for MeNB operation.

6. Simulation Results

In this section we present the simulation results. Section 6.1 evaluates the maximum rate allowed at SeNB for DL transmission according to the expression derived in Section 5.1. Section 6.2 compares the average sum-rate and per-user rate performances of ‘INT’ and ‘SIC’ strategies, based on the developed expressions in Section 5.2. We consider $\bar{\gamma} = 1$, $|h_{\text{SeNB-MeNB}}|^2 = 1$, $\alpha_1 = \{2, 2.5, 3\}$, $\alpha_2 = 3$, $\alpha_3 = 3.5$, $\alpha_4 = 4$, $k_1 = k_2 = k_3 = k_4 = (4\pi/\lambda)^2$, $\lambda = 3 \times 10^8 / 3.5 \times 10^9$ (i.e. 3.5 GHz frequency carrier), $\sigma^2 = 10^{N/10}$, $N = -174 + 10 \log_{10}(2 \times 10^6)$ (i.e. 2 MHz bandwidth and noise spectral density equal to -174 dBm/Hz), $E\{d_{\text{MUE-MeNB}}\} = d_2 = 150$ m, $E\{d_{\text{SeNB-SUE}}\} = d_3 = 20$ m, $E\{d_{\text{MUE-SUE}}\} = d_4 = 100$ m. The MeNB-SeNB distance ($d_{\text{SeNB-MeNB}}$) will be varied through simulations. We use $P_\varepsilon = 0.1$ (i.e. ‘SIC’ strategy is designed in such a way that in 90% of the cases the interference can be decoded at MeNB). Transmit power at MUE (P_{MUE}) equal to 23 dBm is used. For the transmit power at SeNB (P_{SeNB}) we adopt two values: 24 dBm and 30 dBm. A maximum modulation and coding scheme (MCS) is adopted according to LTE.

6.1. Maximum rate at SeNB

Figure 3 displays the maximum rate allowed at the SeNB by following the expression in (11) as a function of the MeNB-SeNB distance ($d_{\text{SeNB-MeNB}}$) for a SeNB transmitted power of 24 dBm (left-figure) and 30 dBm (right-figure). In both cases, different values of the pathloss exponent in the SeNB-MeNB link are displayed ($\alpha_1 = \{2, 2.5, 3\}$). It can be observed that the maximum rate decreases as the MeNB-SeNB distance ($d_{\text{SeNB-MeNB}}$) increases and as the path loss exponent in the SeNB-MeNB link (α_1) increases. Also, the maximum rate decreases as the SeNB transmitted power (P_{SeNB}) decreases. Let us remark that the expression in (11) has been derived for the simplified pathloss model that depends on the pathloss exponent. Nevertheless, the analysis could be properly extended for more sophisticated channel models.

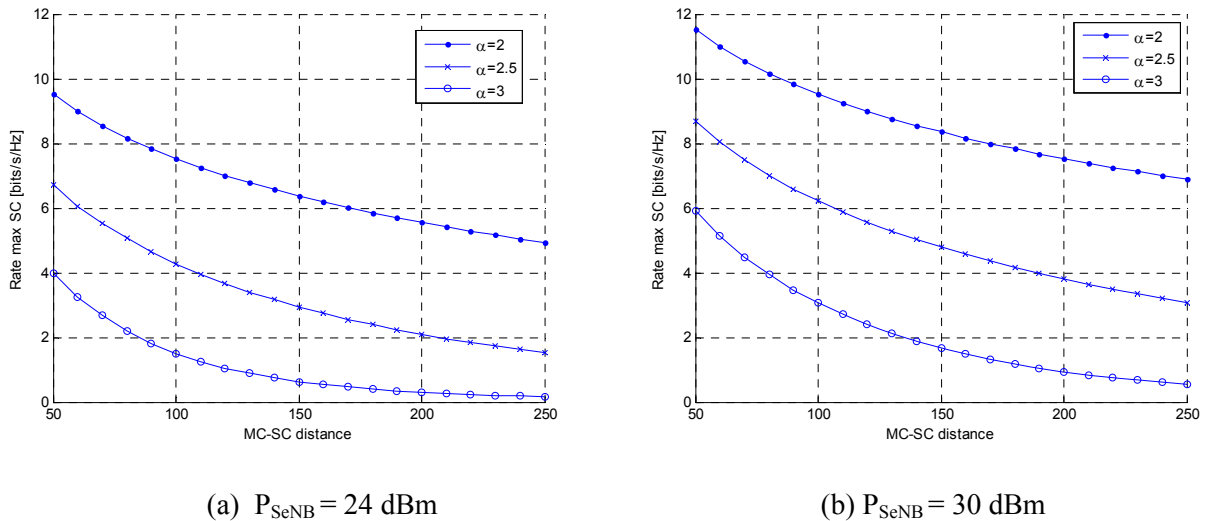
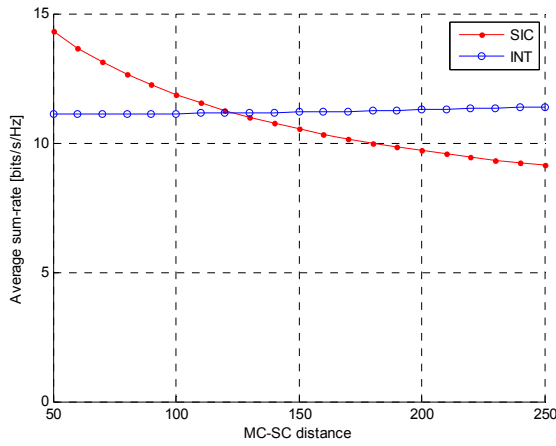


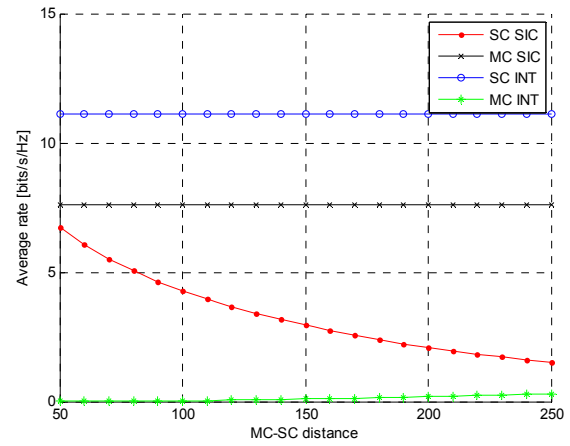
Figure 3. Maximum rate allowed at SeNB (in bits/s/Hz) vs. MeNB-SeNB distance ($d_{\text{SeNB-MeNB}}$, in m) for different values of the SeNB transmitted power (P_{SeNB}) and SeNB-MeNB path loss exponents (α_1).

6.2. Average sum-rate and per-user rate performance

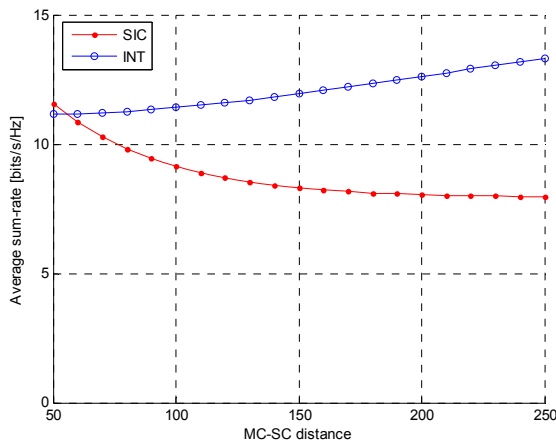
Next figures show the average sum-rate of the users (left-figures) in the scenario shown in Figure 2 and the average rates for the SeNB-SUE link and the MeNB-MUE link, separately, (right-figures) under interference conditions ('INT' in figures, expression SR^{int} in (15)) and SIC assumption ('SIC' in figures, expression SR^{sic} in (15)) as a function of the MeNB-SeNB distance ($d_{\text{SeNB-MeNB}}$). Figure 4 displays the results for a SeNB transmitted power of 24dBm and Figure 5 for a SeNB transmitted power of 30dBm. Two different values of the pathloss exponent in the SeNB-MeNB link are considered: $\alpha_1 = \{2.5, 3\}$.



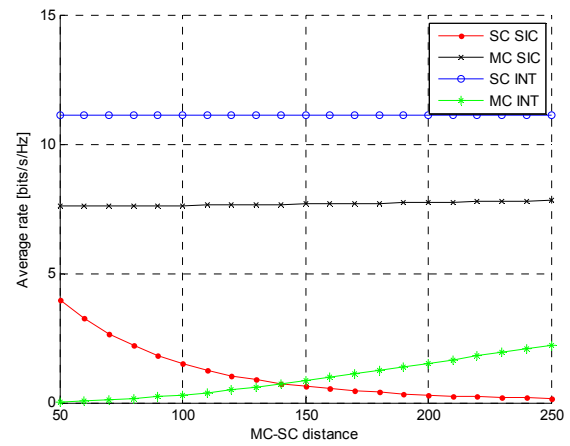
(a) Average sum-rate, $\alpha_1 = 2.5$



(b) Average per-user rate, $\alpha_1 = 2.5$



(c) Average sum-rate, $\alpha_1 = 3$



(d) Average per-user rate, $\alpha_1 = 3$

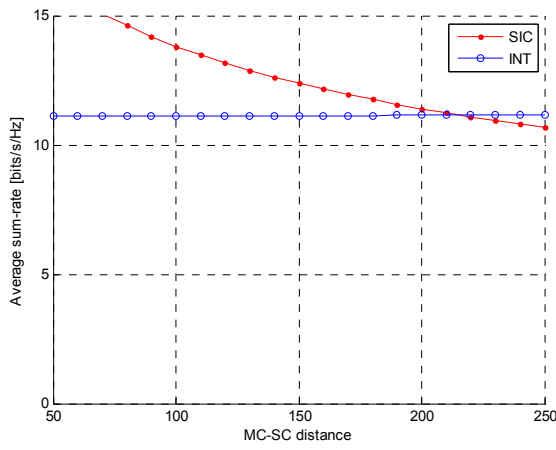
Figure 4. Average sum-rate and average per-user rate (in bits/s/Hz) vs. MeNB-SeNB distance ($d_{\text{SeNB-MeNB}}$, in m) under interference conditions ('INT') and the proposed SIC strategy ('SIC') for $P_{\text{SeNB}} = 24$ dBm and different SeNB-MeNB path loss exponents (α_1).

It can be observed that for low MeNB-SeNB distances, 'SIC' outperforms 'INT' in terms of average sum-rate while for large MeNB-SeNB distances the reverse situation is obtained. There is a threshold distance from which the best strategy in terms of average sum-rate changes. The threshold depends on the SeNB transmitted power and the propagation losses (which are modeled through the

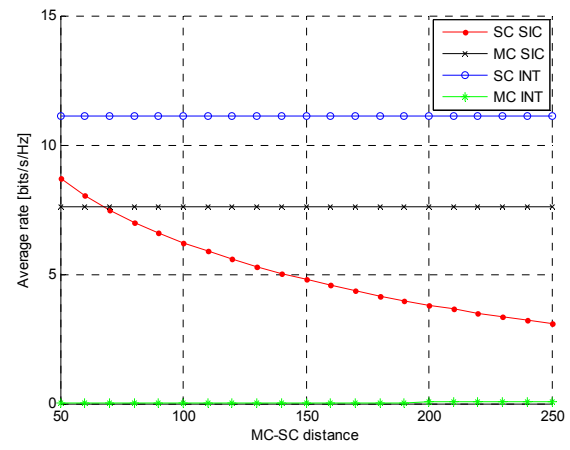
path loss exponent in the SeNB-MeNB link, α_1). In the scenario under consideration with simplified pathloss modelling, the thresholds for MeNB-SeNB distances correspond to:

- 124 m for $P_{\text{SeNB}} = 24$ dBm and $\alpha_1 = 2.5$ (see Figure 4.(a)),
- 55 m for $P_{\text{SeNB}} = 24$ dBm and $\alpha_1 = 3$ (see Figure 4.(c)),
- 215 m for $P_{\text{SeNB}} = 30$ dBm and $\alpha_1 = 2.5$ (see Figure 5.(a)),
- 88 m for $P_{\text{SeNB}} = 30$ dBm and $\alpha_1 = 3$ (see Figure 5.(c)).

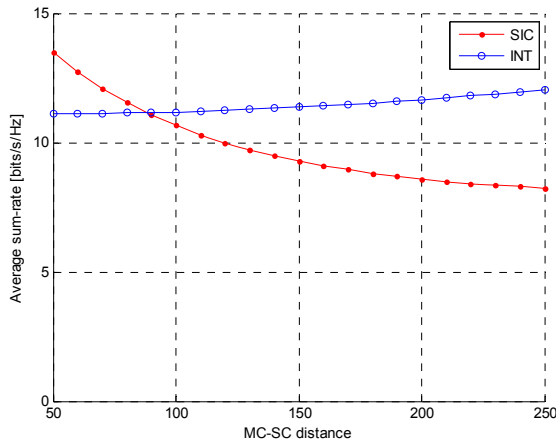
For fixed MeNB-SeNB propagation conditions, if the SeNB transmitted power is increased then the threshold distance is also increased (i.e. ‘SIC’ outperforms ‘INT’ in larger deployment distances). On the other hand, for a fixed SeNB transmitted power, if the MeNB-SeNB propagation conditions are improved (i.e. α_1 is reduced) then the threshold distance is also increased.



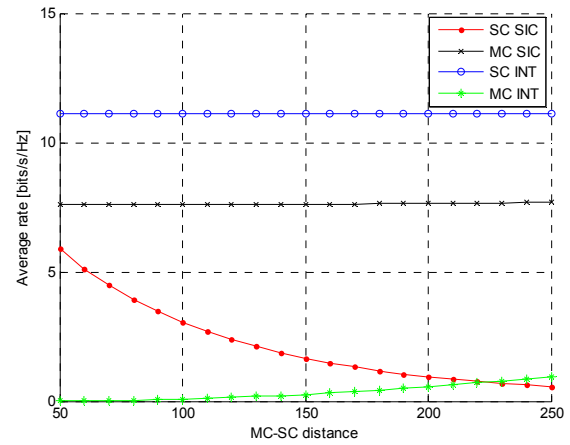
(a) Average sum-rate, $\alpha_1 = 2.5$



(b) Average per-user rate, $\alpha_1 = 2.5$



(c) Average sum-rate, $\alpha_1 = 3$



(d) Average per-user rate, $\alpha_1 = 3$

Figure 5. Average sum-rate and average per-user rate (in bits/s/Hz) vs. MeNB-SeNB distance ($d_{\text{SeNB-MeNB}}$, in m) under interference conditions (‘INT’) and the proposed SIC strategy (‘SIC’) for $P_{\text{SeNB}} = 30$ dBm and different SeNB-MeNB path loss exponents (α_1).

In Figure 4.(b)-(d) and Figure 5.(b)-(d) we can observe the behavior of the different average rates of the users. Under ‘SIC’ strategy, the average rate of the SeNB-SUE link is decreased with the

MeNB-SeNB distance due to the maximum rate allowed at SeNB (as it was shown in Figure 3) while the average rate of the MeNB-MUE link has a high value and a very low increase with respect to the MeNB-SeNB distance because the proposed ‘SIC’ strategy allows decoding the MUE signal interference-free at the MeNB in 90% of the cases (so, interference from the SeNB does not impact on the rate). Under ‘INT’ strategy, the average rate of the SeNB-SUE link does not vary with the MeNB-SeNB distance because the interference comes from the MUE, while the average rate of the MeNB-MUE link has a very low value and is increasing with the MeNB-SeNB distance because the farther the SeNB is the lower interference is received at MeNB.

It is very important to note that the average rate of the MeNB-MUE link is highly degraded due to interference, while the proposed transmit coordination approach for SIC implementation allows a very good rate at the MeNB-MUE link while constraining the SeNB-SUE average rate (i.e. the rate at which an SeNB that attempts to access the licensed FDD-UL band can transmit). Note that the average rate in the SeNB-SUE link corresponds to its maximum MCS under interference conditions for any MeNB-SeNB distance (and for that reason it does not vary with different SeNB transmitted power), because the SUE is placed close to the SeNB and the interference received from the MUE is very low and unlikely. Let us finally remark again that the expressions in (15) have been derived for the simplified pathloss model that depends on the pathloss exponent. However, the analysis could be extended for more sophisticated channel models.

6. Extension to multiple SeNBs

Assume that multiple TDD SeNBs are allowed to reuse the FDD-UL band where the MeNB operates in UL. Let us present, for simplicity, the case where we have just two SeNBs, as shown in Figure 6, although the concept can be easily extended to more than two SeNBs. To implement successive interference decoding and suppression at the MeNB it is convenient to have SeNBs at different distances (e.g. in Figure 6, SeNB 1 is closer to the MeNB than SeNB 2) such that the SeNBs can be ordered. Under this ordering, we will limit the transmission rate of the different SeNBs as follows.

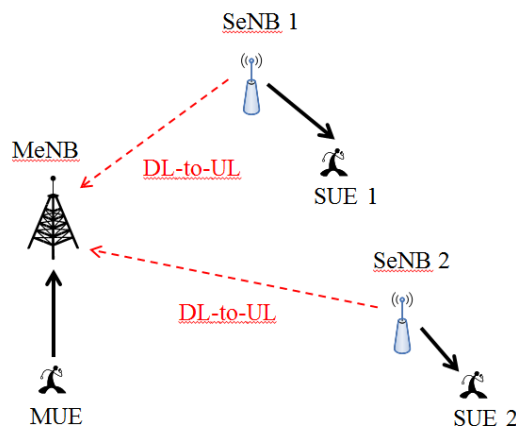


Figure 6. Extended scenario, composed of a MeNB receiving in UL and multiple SeNBs transmitting in DL. Interference suppression strategies are implemented at the MeNB to decode and suppress the signals received from the different SeNBs, successively.

First, SeNB 1 will need to be decoded with interference from SeNB 2 and MUE. So, we will limit its transmission rate such that in 90% of the cases the SeNB 1 signal can be decoded at the MeNB (assuming interference from SeNB 2 and MUE). Next, if decoding is successful, the signal from SeNB 1 will be subtracted from the received signal at the MeNB. Then, SeNB 2 signal will need to be decoded with interference from the MUE, such that we will limit its transmission rate in a way that in 90% of the cases the SeNB 2 signal can be decoded at the MeNB (assuming interference from MUE). Finally, if decoding is also successful, the signal from SeNB 2 will be subtracted from the received signal at the MeNB and the MUE signal could be decoded without interference.

This would be the way to proceed, i.e. by limiting the transmission rate of all SeNBs that cause major interference towards the MeNB, successively. Note that as more SeNBs coexist in the FDD UL band, more interference would be present to decode the signal from the first SeNB in the ordering. Thus, the rate of the closest SeNB would be the one more restricted. In this sense, the more SeNBs are allowed to transmit, the higher the sum-rate is increased but the lower are the individual transmission rates allowed at the SeNBs that are closer to the MeNB. Notice that this scenario is akin to the Multiple Access Channel [10].

7. Conclusion

In this paper we have proposed a coordinated strategy to limit the SeNB's transmission rate when the TDD SeNB is allowed to access the FDD-UL band of a MeNB. The rate limitation is made such that decoding of the SeNB data symbols at the MeNB is possible and hence it allows decoding of the useful MUE signal interference-free. The proposed approach constrains the rate of the SeNB but keeps nearly normal operation of the MeNB in the FDD-UL band. Extension to the case where multiple TDD SeNBs are deployed within the MeNB coverage areas is also analyzed.

The use of successive interference decoding and suppression at the MeNB through the limitation of the SeNB transmission rate for DL has been shown to provide gains in terms of average sum-rate as compared to a fully opportunistic access in two non-exclusive situations: when the SeNB is close to the MeNB and when the SeNB transmits at high power (i.e. high interference conditions). Otherwise, if the SeNB is far apart from the MeNB and uses low power, the average sum-rate under interference conditions without considering interference decoding and suppression provides a larger average sum-rate gain; however, the individual average rates of the MUEs are still degraded due to interference and normal MeNB operation is not maintained. This is resolved with the proposed strategy.

Acknowledgements

This work has been supported by Huawei Technologies Co. Ltd.

References

- [1] Qualcomm: Wireless broadband future and challenges, Oct. 2010.
- [2] DIGITALEUROPE: Call For Timely Harmonisation of the 1452-1492MHz and 2300-2400MHz Bands to Support Delivery of EU Radio Spectrum Policy Programme Objectives, Brussels, Feb. 2012.
- [3] N. Bhushan *et al.*, "Network densification: the dominant theme for wireless evolution into 5G," IEEE Commun. Mag., vol. 52, pp. 82–89, Feb. 2014.
- [4] A. Agustin *et al.*, "Efficient use of paired spectrum bands through TDD small cell deployments", accepted for publication at IEEE Commun. Mag., May 2017. Draft version available at <https://arxiv.org/abs/1612.02175>
- [5] 3GPP TR 36.882, "Study on regulatory aspects for flexible duplex for EUTRAN", Release 13, Sep. 2015.
- [6] 3GPP R1-134295, "FDD-TDD CA/Dual Connectivity solution exploiting traffic asymmetry in duplex-neutral bands", Oct. 2013.
- [7] S. Lagen *et al.*, "Long-term provisioning of radio resources based on their utilization in dense OFDMA networks", IEEE Int. Symp. on Personal, Indoor and Mobile Radio Communications., Valencia (Spain), Sep. 2016.
- [8] 3GPP TR 36.866, "Study on Network-Assisted Interference Cancellation and Suppression (NAIC) for LTE", v12.0.1, Mar. 2014
- [9] 3GPP TR 36.828, "Further enhancements to LTE Time Division Duplex (TDD) for Downlink-Uplink (DL-UL) interference management and traffic adaptation", v11.0.0, Jun. 2012.
- [10] D. Tse, P. Viswanath, Fundamentals of Wireless Communications, Cambridge University Press, 2005